

# Enhancing Skin Cancer Detection Using Hybrid Deep Neural Network (HDNN) Approach

Nitin Kumar<sup>1\*</sup>, Vipin Kataria<sup>2\*\*</sup>

<sup>1</sup> Independent Researcher 0009-0001-2370-3492, <sup>2</sup> Independent Researcher 0009-0006-5332-7965

\* [nitink3@illinois.edu](mailto:nitink3@illinois.edu), [vkataria@picarro.com](mailto:vkataria@picarro.com)

+ These authors contributed equally to this work

## Abstract

Skin cancer remains one of the most aggressive and potentially fatal forms of cancer worldwide. Its early detection is paramount, as timely diagnosis significantly enhances the likelihood of successful treatment and long-term survival. However, traditional diagnostic methods often require expert dermatological assessment, which may not always be readily available, especially in resource-constrained environments. To address this challenge, we present a novel skin cancer detection framework based on a Hybrid Deep Neural Network (HDNN) architecture. The proposed model integrates the strengths of multiple deep learning paradigms to achieve robust feature extraction and classification. It was rigorously evaluated using a publicly available dermoscopic image dataset and achieved a maximum classification accuracy of 87.33% on the test set. In addition to presenting the architecture and performance of the HDNN, we conducted a comparative analysis with several state-of-the-art models, including DenseNet201, EfficientNetB0, MobileNet, and ResNet152. The results demonstrate that our HDNN model outperforms these baselines in terms of both accuracy and consistency. The improved diagnostic precision achieved through our approach has significant implications for clinical practice, as it can enable faster, more reliable screening of skin lesions. Ultimately, this could contribute to earlier interventions, reduced treatment costs, and improved patient outcomes. Our findings highlight the potential of deep learning in advancing skin cancer diagnostics.

**Keywords:** skin-cancer, machine learning, deep neural network, CNN.

## 1. INTRODUCTION

Skin cancer mortality rates worldwide are influenced by a complex interplay of factors, including ultraviolet (UV) radiation exposure, demographic characteristics, healthcare access, and socioeconomic conditions. UV radiation is the primary risk factor for skin cancer, with increased exposure leading to higher incidence and mortality rates, particularly in regions with intense sunlight such as Australasia, North America, and Europe [1] [2] [3]. The incidence of skin cancer is notably higher in fair-skinned populations due to their lower melanin levels, which provide less natural protection against UV radiation [4] [3]. Additionally, socioeconomic factors, as measured by the Human Development Index (HDI), play a significant role; countries with higher HDI often report higher incidence rates due to better diagnostic capabilities and increased UV exposure from lifestyle choices, yet they may experience lower mortality rates due to better healthcare access [1] [5]. Conversely, regions with lower HDI, such as parts of Africa and Asia, may have lower incidence rates but higher mortality rates due to limited access to healthcare and early detection services [1] [6]. The mortality rate is also influenced by the

type of skin cancer, with non-melanoma skin cancers (NMSC) causing more deaths globally than melanoma, despite melanoma being more aggressive, due to the sheer volume of NMSC cases [7] [8]. Furthermore, disparities in healthcare access, particularly in tropical regions with limited resources, exacerbate mortality rates as early detection and treatment are less accessible [4]. The increasing global burden of skin cancer necessitates enhanced preventive measures, such as public education on UV protection and improved healthcare infrastructure to facilitate early diagnosis and treatment [6] [8]. Overall, addressing these multifaceted factors is crucial for reducing skin cancer mortality rates worldwide.

The current gaps in skin cancer diagnosis that lead to delayed or inaccurate detection are multifaceted, involving provider, patient, and systemic barriers. A significant issue is the shortage of dermatologists, which forces primary care physicians (PCPs) to fill the gap, despite many lacking the necessary dermatologic training and time to conduct thorough skin examinations [9] [10]. This lack of expertise among PCPs often results in missed detection opportunities and incorrect reassurances to patients about suspicious lesions [10]. Additionally, the reliance on traditional diagnostic techniques, which are complex and expensive, further complicates early detection efforts [11]. Patients also contribute to delays, often due to low perceived risk, lack of knowledge about melanoma, and long wait times for appointments [9] [12]. Many patients delay seeking medical attention, with some waiting over 12 months after noticing changes in a lesion [12] [13]. Misdiagnosis is another critical issue, particularly with atypical presentations of melanoma, such as acral melanoma, which can mimic benign conditions like warts or infections [14]. Furthermore, systemic issues such as inadequate public awareness, lack of reimbursement for preventive care, and insufficient collaboration between specialists and PCPs exacerbate these challenges [10] [15]. Technological advancements, such as deep learning models, offer potential solutions by improving diagnostic accuracy and reducing reliance on human interpretation, yet their integration into clinical practice remains limited [16]. Overall, addressing these gaps requires a comprehensive approach involving enhanced training for PCPs, public education, improved access to dermatologic care, and the adoption of advanced diagnostic technologies [9] [17] [16].

## 2. LITERATURE SURVEY

Machine learning has emerged as a transformative tool in the early detection and diagnosis of skin cancer, particularly melanoma, which is known for its high mortality rate if not identified early. Various studies have demonstrated the efficacy of machine learning algorithms in distinguishing between malignant and benign skin lesions, thereby enhancing diagnostic accuracy and patient outcomes. Convolutional Neural Networks (CNNs) have been highlighted as particularly effective, achieving high accuracy, sensitivity, and specificity in skin cancer detection tasks. For instance, CNNs have been reported to achieve accuracy rates as high as 92.5% in some studies, outperforming traditional machine learning models like Support Vector Machines (SVMs) and Random Forests [18] [19]. The integration of deep learning models with traditional machine learning techniques, such as the use of transfer learning models for feature extraction followed by classification using algorithms like Random Forest, has also shown promising results, achieving accuracy rates over 90% [20]. Despite these advancements, challenges such as model interpretability, dataset diversity, and the need for extensive datasets remain. Addressing these issues is crucial for the practical implementation of these models in clinical settings [21] [19]. Moreover, the use of large datasets, such as those from the International Skin Imaging Collaboration (ISIC), has been instrumental in training robust models capable of generalizing across diverse populations [22]. The potential of machine

learning in skin cancer diagnostics is further underscored by its ability to automate and streamline the diagnostic process, reducing reliance on subjective human interpretation and potentially improving healthcare accessibility, especially in resource-constrained settings [18] [23]. As research continues to refine these algorithms and expand their applicability, the integration of machine learning into dermatological practice holds significant promise for enhancing early detection and improving patient care outcomes [24].

Deep learning techniques, particularly Convolutional Neural Networks (CNNs), play a pivotal role in the detection and classification of skin cancer by offering high accuracy and efficiency in image analysis. These techniques are adept at identifying subtle differences in skin lesions, which is crucial for early detection and treatment of skin cancer, including basal cell carcinoma, squamous cell carcinoma, and melanoma [25] [26]. The use of CNNs, often enhanced with advanced techniques such as Batch Normalization, Max Pooling, and dropout layers, helps prevent overfitting and improves the accuracy of skin cancer classification systems [26]. The integration of deep learning models with large datasets, such as the HAM10000 and ISIC datasets, allows for the training of models that can generalize well across different lesion types, thereby enhancing classification accuracy [27] [28] [29]. Techniques like data augmentation and transfer learning further improve model performance by increasing sample diversity and leveraging pre-trained models for better feature extraction [28] [30]. Additionally, the use of deep learning models such as ResNet, VGG, and GoogLeNet, along with innovative architectures like Capsule Neural Networks (CapsNet) and Gabor Capsule Networks (GCN), have shown promising results in achieving high accuracy rates, with some models reaching up to 98.4% accuracy [28] [31] [32]. These advancements not only facilitate more accurate and automated classification of skin lesions but also support healthcare professionals by providing reliable diagnostic tools that can be integrated into clinical practice, potentially through web-based or mobile applications for broader accessibility [26] [30]. Overall, deep learning techniques significantly enhance the early detection and classification of skin cancer, contributing to improved patient outcomes and more efficient healthcare delivery [33] [32].

### 3. PROPOSED SYSTEM

[Fig. 1](#) is workflow of the proposed approach. The process begins with splitting the data into training and test. The training data is used to train the HDNN network and test data is used to test the trained model performance using standard classification metrics: Accuracy, F1-Score, Precision, Recall and AUC-ROC as shown in [Table I](#).

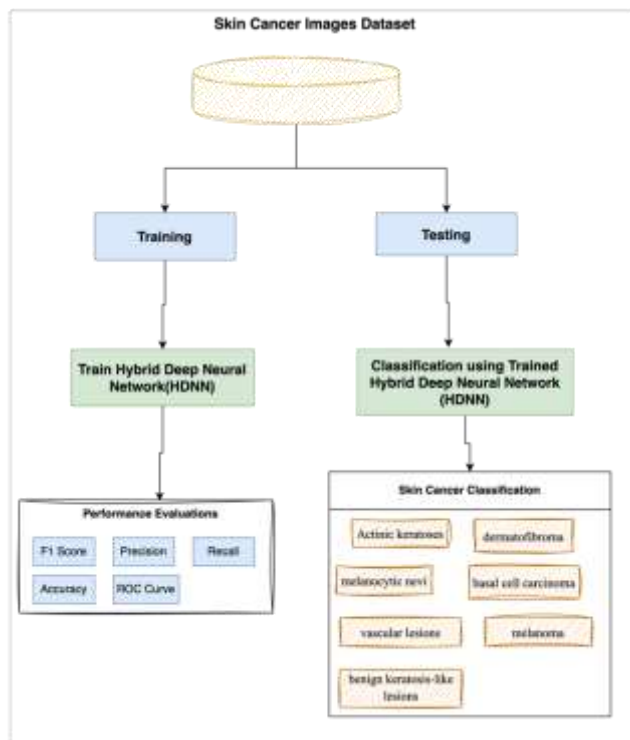


Fig.1 Workflow of the proposed approach.

#### Dataset

The data set used in the current study is from HAM10000 dataset and can be accessed publicly on the following URL [17]. The data set consists of 10000 dermoscopic images of skin lesions. The images have size 650X450 and it represents collection of all important diagnostic categories in the realm of pigmented lesions: Actinic keratoses and intraepithelial carcinoma / Bowen's disease (akiec), basal cell carcinoma (bcc), benign keratosis-like lesions (solar lentiginos / seborrheic keratoses and lichen-planus like keratoses, bkl), dermatofibroma (df), melanoma (mel), melanocytic nevi (nv) and vascular lesions (angiomas, angiokeratomas, pyogenic granulomas and hemorrhage, vasc).

#### Performance Metrics

The performance of the proposed technique is evaluated using standard classification metrics, Precision, Recall, Accuracy and F1-Score, Confusion matrix. In classification tasks involving images, the terms TP (True Positive), TN (True Negative), FP (False Positive), and FN (False Negative) are used to evaluate the classifier's performance. The terms "True" and "False" indicate whether the classifier's prediction aligns with the actual classification, while "Positive" and "Negative" refer to the classifier's prediction. The calculation methods for these metrics are detailed below

Accuracy is the proportion of all classifications that were correct, whether positive or negative.

$$Accuracy = \frac{TP + FP}{TP + FP + FN + TN}$$

The false positive rate (FPR) is the ratio of false positives (FP) to the total number of actual negatives (FN + TN)

$$FPR = \frac{FP}{TN + FP}$$

The true positive rate (TPR) is the ratio of TP to the total number of actual positive (FN + TP)

$$TPR = \frac{TP}{FN + TP}$$

Precision is the ratio of the correctly classified actual positives to the everything classified as positive.

$$Precision = \frac{TP}{TP + FP}$$

Recall is the proportion of all actual positives that were classified correctly as positives.

$$Recall = \frac{TP}{TP + FN}$$

'F1 Score' or 'F-measure' is a measure that combines precision, and recall is the harmonic mean of precision and recall.

$$F1\ Score = \frac{2 * precision * recall}{precision + recal}$$

### *Data Splitting*

The dataset was balanced using computed class weights to address the inherent class imbalance in skin lesion classifications. Using stratified sampling to maintain class distribution, the data was split into training (80%), validation (10%), and test (10%) sets. The stratification was performed based on the class labels to ensure representative distribution of all skin conditions across the splits. This systematic splitting approach helps maintain statistical validity while preserving sufficient samples for model training and evaluation.

### *Train the Hybrid Neural network*

The train data is feed to the Hybrid Deep Neural Network (HDNN). [Fig. 2](#) shows the HDNN architecture.

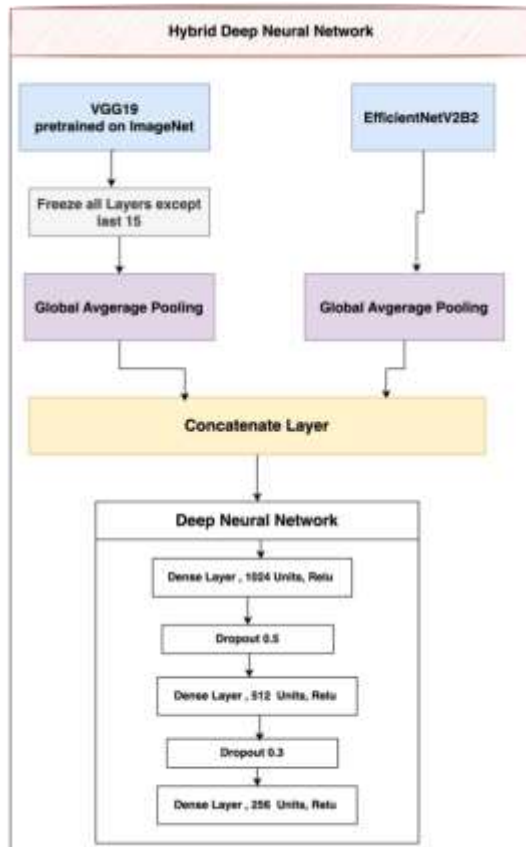


Fig. 2 Architecture of Hybrid Deep Neural Network(HDNN).

The proposed Hybrid Deep Neural Network (HDNN) architecture synergistically combines the strengths of VGG19 and EfficientNetV2B2 networks for skin cancer detection. The processed images are feed to a truncated version of VGG19 which is pretrained on the ImageNet dataset. All layers marked as untrainable except last 15 layers to take advantage of transfer learning. In parallel, train data also feed to EfficientNetV2B2 architecture for efficient high-level feature extraction. Both networks process the input images independently before their outputs undergo Global Average Pooling and subsequent concatenation, creating a rich, multi-scale feature representation. This combined feature set is then processed through a carefully designed Deep Neural Network head, comprising three dense layers (1024, 512, and 256 units) with ReLU activation and strategic dropout rates (0.5 and 0.3) to prevent overfitting. The architecture culminates in a 7-unit SoftMax layer for final classification. The model is optimized using Adam optimizer with a learning rate of 0.0001 and implements class weights to handle potential data imbalances. This hybrid approach enables comprehensive feature extraction at multiple scales while maintaining computational efficiency, making it particularly effective for the complex task of skin cancer detection.

### Models

Below are the details of the models tried in the current study.

DenseNet201: Densenet201 is a deep convolutional neural network (CNN) with 201 layers,

distinguished by its dense connectivity architecture. In this design, each layer receives feature maps from all preceding layers within a block, which significantly enhances feature reuse and reduces the number of parameters required. This architecture includes dense blocks, where the dense connectivity occurs, and transition layers, which help in down sampling the feature maps and reducing spatial dimensions. Densenet201 is widely applied in image recognition tasks, including medical diagnosis, such as detecting laryngeal cancer, and plant disease detection, like identifying leaf diseases. The model's ability to extract rich features and its high accuracy make it a preferred choice for these applications. Additionally, Densenet201 often leverages pre-trained weights from ImageNet to improve its performance in specific tasks, allowing for efficient fine-tuning and adaptation to new datasets.

**EfficientNetB0:** It is the base model in the EfficientNet family, introduced by Google AI in 2019. It uses a novel compound scaling method to balance depth, width, and resolution, achieving state-of-the-art accuracy with significantly fewer parameters and computational requirements compared to traditional architectures. EfficientNetB0 employs Mobile Inverted Bottleneck (MBConv) layers combined with Squeeze-and-Excitation (SE) blocks to enhance feature extraction and focus on essential features. The model has an input resolution of 224x224 and is pre-trained on ImageNet, making it suitable for transfer learning tasks. EfficientNetB0 is widely used for image classification, object recognition, and medical imaging applications due to its efficiency and adaptability across various computational budgets.

**MobileNet:** It is a lightweight convolutional neural network (CNN) designed for mobile and embedded vision applications. It was developed by Google to efficiently run on devices with limited computational resources, such as smartphones. The architecture primarily uses depth wise separable convolutions, which significantly reduce the number of parameters and computational cost compared to standard convolutions. This approach allows MobileNet to achieve high accuracy while being much smaller and faster than other models.

**ResNet152:** It is a deep convolutional neural network (CNN) that features 152 layers and is part of the ResNet family, which introduced residual learning to combat the vanishing gradient problem in very deep networks. The architecture employs residual blocks with shortcut connections, allowing the network to learn identity mappings and significantly improving training efficiency and accuracy. Pre-trained on large datasets like ImageNet, ResNet152 achieves impressive performance with top-1 and top-5 error rates of 21.69% and 5.94%, respectively. This model is widely used in image classification tasks and supports transfer learning, making it adaptable for various applications, including medical imaging and object detection.

#### **4. RESULTS AND DISCUSSION**

Below are the results from our proposed approach along with comparison against others Deep Neural Networks (DenseNet201, EfficientNetB0, MobileNet, Resnet152).

[Fig. 3](#) illustrates the training performance of models, displaying significantly higher scores across all metrics compared to the test set. MobileNet performs best in training data across all the metrics, it reaches a 99.74% accuracy, 99.70% with F1 score, 99.68% on recall and 99.71% on precision. It's followed by EfficientNetB0, with 99.61% accuracy, 99.51% with F1 score, 99.69% on recall and 99.34% on precision. HDNN performs little lower with the above two with 99.58% accuracy, 99.13% with F1 score, 99.45% on recall and 99.83% on precision. ResNet152 performs consistently lower around 5% compared with top models. DenseNet201 shows 97.36% accuracy, 93.17% with F1 score, 91.36% on recall and 96.16% on precision.

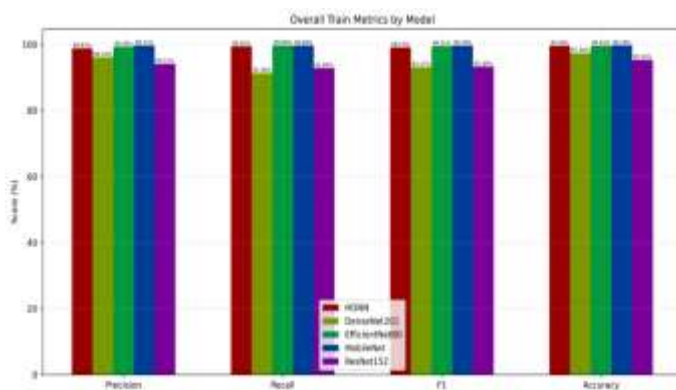


Fig. 3. Performance Metrics by Model on Train data

[Fig. 4](#) presents the overall test performance metrics, including Precision, Recall, F1-score, and Accuracy, for HDNN, DenseNet201, EfficientNetB0, MobileNet, and ResNet152. The results indicate that HDNN consistently outperforms the other architectures across all metrics, achieving the highest Recall (80.42%), F1-score (79.54%), Precision (79.55%) and Accuracy (87.33%). EfficientNetB0 and DenseNet201 exhibit competitive performance, with EfficientNetB0 showing superior recall (77.46%) over DenseNet201 (67.92%), suggesting its capability in identifying positive cases more effectively. However, MobileNet and ResNet152 exhibit relatively lower recall values, which could indicate a trade-off between model complexity and generalization. These findings suggest that HDNN is the most effective model for the given classification task.

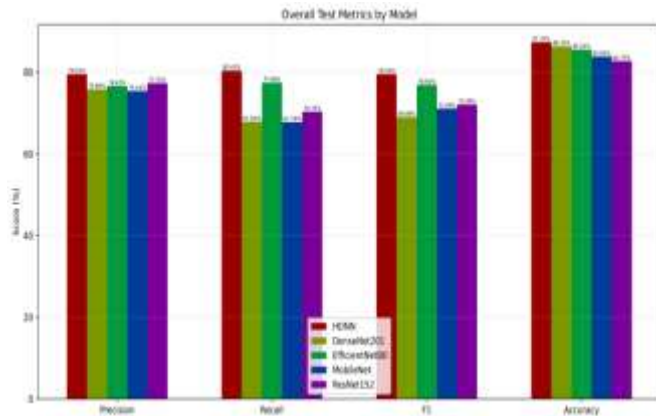


Fig. 4. Performance Metrics by Model on Test data

Fig. 5 shows the confusion matrix for the HDNN train shows the performance of the model in classifying different types of skin cancer. For “bkl”, the model correctly classified 263 instances as “bkl”, but it misclassified 1 instance as “mel”. In the case of “mel”, the model accurately identified 415 instances as “mel”, while 2 instances were incorrectly classified as “akiec”. For “nv”, the model correctly classified 869 instances, but it misclassified 21 instances as 7 as “bkl”, 4 as “mel”, 2 as “vasc”, 1 as “df” and 7 as “akiec”. “vasc” had all 93 correct classifications. “df” saw 897 correct classifications, but 5 instances were misclassified, 1 as “bkl”, 1 as “nv” and 3 as “akiec”. “akiec” had 5425 correct classifications, with 5 instances incorrectly classified, 1 as “vasc” and 4 as “df”. Finally, “bcc” had all 115 correct classifications. This breakdown highlights the model's strengths in correctly identifying most instances, while also pointing out specific areas where it struggled, particularly with distinguishing between nv.



Fig. 5. Confusion Metric HDNN – Train Data

Fig. 6 shows the confusion matrix for the HDNN test results shows the performance of the model in classifying different types of skin cancer. For “bkl”, the model correctly classified 27 instances as “bkl”, but it misclassified 3 instances as “mel” 1 as “nv”, 1 as “vasc” and 1 as akiec. In the case of “mel”, the model accurately identified 39 instances as “mel”, while 2 instances were incorrectly classified as “bkl”, 8 instances as “akiec”, 1 instance as “df”, and 1 instances as “bcc”. For “nv”, the model correctly classified 69 instances as “nv”, but it misclassified 7 as “bkl”, 8 as “mel”, 1 as “vasc”, 9 as “df”, 16 as “akiec”.

For “vasc”, the model correctly classified 10 instances, but it misclassified 1 as “df” and 1 as “akiec”. For “df” the mode correctly classified 69, but misclassified 4 as “bkl”, 1 as “mel”.

This breakdown highlights the model's strengths in correctly identifying most instances, while also pointing out specific areas where it struggled, particularly with distinguishing between “mel”.



Fig. 6. Confusion Metric HDNN – Test Data

The training set ROC curves as depicted in Fig. 7 exhibit perfect classification performance across all seven classes, with Area Under the Curve (AUC) values of 1.00 uniformly. This indicates optimal model convergence during the training phase, successfully capturing the distinctive features of each skin lesion condition.

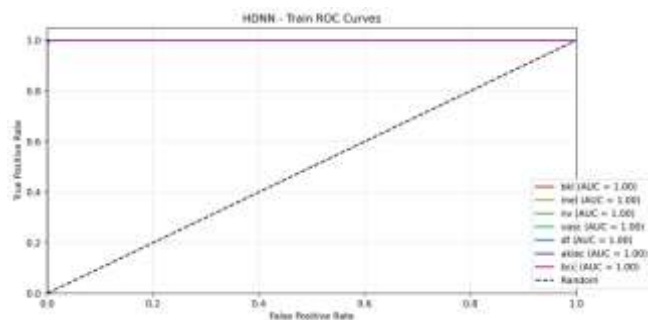
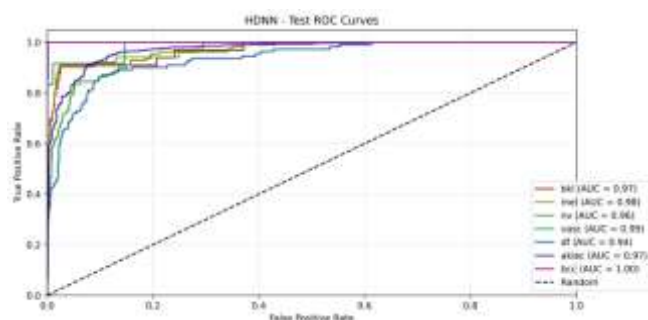


Fig. 7. HDNN ROC Curve – Train Data

Our evaluation of the test set ROC curves [Fig. 8](#) reveals exceptional generalization performance across all dermatological classes. The model demonstrates particularly impressive results for detecting “bcc”, achieving perfect classification with an AUC of 1.00. This is closely followed by highly accurate identification of “vasc” (AUC = 0.99) and “mel” (AUC = 0.98). The model also performs admirably in distinguishing both “bki” and “akiec”, with both conditions achieving an AUC of 0.97. Detection of “nv” maintains strong reliability with an AUC of 0.96, while “df” classification shows robust performance with an AUC of 0.94. These comprehensive results demonstrate the model's strong discriminative capabilities across all classes, with no class falling below an AUC threshold of 0.94.



## 5. CONCLUSION

In conclusion, this study presents a robust and innovative approach to skin cancer detection through the development of a Hybrid Deep Neural Network (HDNN) that integrates the strengths of VGG19 and EfficientNetV2B2 architectures. By leveraging transfer learning, multi-scale feature extraction, and a carefully designed classification head, the HDNN model demonstrates superior performance across multiple evaluation metrics, achieving a test accuracy of 87.33% and outperforming established models such as DenseNet201, EfficientNetB0, MobileNet, and ResNet152. The use of the HAM10000 dataset, along with stratified sampling and class balancing techniques, ensures the model's generalizability and fairness across diverse lesion types. The comprehensive evaluation, including confusion matrices and ROC curves, highlights the model's strong discriminative capabilities, particularly in identifying challenging classes like melanoma and basal cell carcinoma. The proposed HDNN model holds significant promise for real-world clinical integration. Its ability to accurately classify various types of skin lesions can support dermatologists in making faster

and more reliable diagnoses. In resource-limited settings, where access to dermatological expertise is scarce, this model could be deployed via mobile or web-based platforms to facilitate early screening. Such tools can empower primary care providers and even patients to identify suspicious lesions, prompting timely medical intervention. By reducing diagnostic delays and minimizing human error, the HDNN model can contribute to improved patient outcomes and reduced healthcare costs.

Despite the promising results, this study has several limitations. First, the model was trained and evaluated on the HAM10000 dataset, which, while comprehensive, may not fully represent the diversity of skin tones and lesion types encountered in global clinical settings. Second, the model's performance in real-world scenarios—such as varying image quality, lighting conditions, and device types—remains untested. Additionally, the black-box nature of deep learning models poses challenges for clinical interpretability, which may hinder adoption by healthcare professionals. Addressing these limitations is essential for broader clinical deployment.

Future research will focus on enhancing the model's interpretability through explainable AI techniques, enabling clinicians to understand the rationale behind predictions. Expanding the dataset to include more diverse populations and real-world images will improve generalizability. Moreover, integrating patient metadata (e.g., age, lesion history) alongside image data could further refine diagnostic accuracy. Finally, deploying the model in a pilot clinical setting or as part of a teledermatology platform will help assess its practical utility and user acceptance.

## REFERENCES

- [1] M. Wang, X. Gao, and L. Zhang, "Recent global patterns in skin cancer incidence, mortality, and prevalence," *Chinese Medical Journal*, Dec. 2024, doi: 10.1097/cm9.00000000000003416.
- [2] U. Leiter, U. Keim, and C. Garbe, "Epidemiology of Skin Cancer: Update 2019," Jan. 2020, doi: 10.1007/978-3-030-46227-7\_6.
- [3] R. N. Saladi and A. N. Persaud, "The causes of skin cancer: a comprehensive review.," *Drugs of Today*, Jan. 2005, doi: 10.1358/DOT.2005.41.1.875777.
- [4] P. Couppié and A. Traoré, "Cutaneous Cancers (Including Melanoma)," Jan. 2015, doi: 10.1007/978-3-319-18257-5\_42.
- [5] A. Mohammadbeigi, S. Khazaei, Y. Veisani, A. Delpisheh, and E. Jenabi, "Global inequality in the incidence and mortality rate of melanoma skin cancer according to human development index: a country-level analysis," Jan. 2021, doi: 10.4103/EJDV.EJDV\_10\_20.
- [6] S. Federico, F. Fortarezza, G. Ingravallo, and G. Cazzato, "Epidemiology of Skin Cancer in 2024," Jan. 2025, doi: 10.5772/intechopen.1008698.
- [7] C. W. Rundle et al., "Epidemiologic Burden of Skin Cancer in the US and Worldwide," *Current Dermatology Reports*, Dec. 2020, doi: 10.1007/S13671-020-00311-4.
- [8] W. Zhang et al., "Global, regional and national incidence, mortality and disability-adjusted life-years of skin cancers and trend analysis from 1990 to 2019: An analysis of the Global Burden of Disease Study 2019.," *Cancer Medicine*, Jun. 2021, doi: 10.1002/CAM4.4046.

- [9] M. Najmi, A. E. Brown, S. R. Harrington, D. Farris, S. Sepulveda, and K. C. Nelson, "A systematic review and synthesis of qualitative and quantitative studies evaluating provider, patient, and health care system-related barriers to diagnostic skin cancer examinations," *Archives of Dermatological Research*, Apr. 2021, doi: 10.1007/S00403-021-02224-Z.
- [10] R. C. Wender, "Barriers to effective skin cancer detection.," *Cancer*, Jan. 1995, doi: 10.1002/1097-0142(19950115)75:2+<691::AID-CNCR2820751412>3.0.CO;2-G.
- [11] "Skin Cancer Detection Using Computer Vision," Jan. 2022, doi: 10.1007/978-981-19-0745-6\_1.
- [12] M. Schmid-Wendtner, J. Baumert, J. Stange, and M. Volkenandt, "Delay in the diagnosis of cutaneous melanoma: an analysis of 233 patients.," *Melanoma Research*, Aug. 2002, doi: 10.1097/00008390-200208000-00012.
- [13] S. M and R. E, "Delay in the diagnosis of malignant melanoma," *Harefuah*, Oct. 1989.
- [14] M. Scalvenzi, F. Palmisano, and C. C, "Misdiagnosed, Mistreated And Delay Diagnosed Acral Melanoma: The Atypical Presentations," *Journal of clinical & experimental dermatology research*, Jan. 2012, doi: 10.4172/2155-9554.S6-002.
- [15] M. Gajda and G. Kamińska-Winciorek, "Do Not Let to Be Late: Overview of Reasons for Melanoma Delayed Diagnosis," *Asian Pacific Journal of Cancer Prevention*, Jan. 2014, doi: 10.7314/APJCP.2014.15.9.3873.
- [16] P. Thapar and S. Tiwari, "Empowering Skin Cancer Diagnosis: Integrating Advanced Deep Learning Models with Explainable AI for Lesion Classification," Aug. 2024, doi: 10.1109/iceect61758.2024.10739236.
- [17] K. Nguyen, A. C. Geller, and J. Y. Lin, "Improvements and continued challenges in the early detection of skin cancers," *Expert Review of Dermatology*, Oct. 2012, doi: 10.1586/EDM.12.46.
- [18] A. Nguyen, R. M. Jewel, and A. Akter, "Comparative Analysis of Machine Learning Models for Automated Skin Cancer Detection: Advancements in Diagnostic Accuracy and AI Integration," *The American journal of medical sciences and pharmaceutical research*, Jan. 2025, doi: 10.37547/tajmspr/volume07issue01-03.
- [19] A. Nguyen, M. S. Shak, and M. Al-Imran, "Advancing early skin cancer detection: a comparative analysis of machine learning algorithms for melanoma diagnosis using dermoscopic images," *International Journal of Medical Science and Public Health Research*, Dec. 2024, doi: 10.37547/ijmsphr/volume05issue12-10.
- [20] Y. Doğan and C. Özdemir, "Enhancing Skin Cancer Diagnosis through the Integration of Deep Learning and Machine Learning Approaches," *Bilişim Teknolojileri Dergisi*, Oct. 2024, doi: 10.17671/gazibtd.1484037.
- [21] S. Chen, "Exploring the application of machine learning for skin cancer image identification," *Advances in engineering innovation*, Sep. 2024, doi: 10.54254/2977-3903/11/2024108.
- [22] Y.-G. Wei, D. Zhang, A. Mulati, and C. Zheng, "Skin Cancer Detection Based on Machine Learning," *Online*, Jun. 2024, doi: 10.60087/jklst.vol3.n2.p86.
- [23] R. Chandragiri, D. K. Reddy, K. S. P. Badarla, A. Syed, K. Modepalli, and K. Sadam, "A Systematic Review on Machine Learning Techniques Used for Early Detection of Skin Cancer," Apr. 2024, doi: 10.1109/csnt60213.2024.10545938.

- [24] M. N. Sharad, Z. M. Sharad, S. L. Anwar, and P. J., "MalenoCare - Skin Cancer Detection and Prescription using CNN and ML," *International Journal of Advanced Research in Science, Communication and Technology*, Nov. 2024, doi: 10.48175/ijarsct-22173.
- [25] C. Kavitha, S. Priyanka, M. P. Kumar, and V. Kusuma, "Skin Cancer Detection and Classification using Deep Learning Techniques," *Procedia Computer Science*, Jan. 2024, doi: 10.1016/j.procs.2024.04.264.
- [26] K. N. Premnath, P. Sundaravadivel, A. R., K. Srimathi, M. Vaishnavi, and N. Sathya, "Deep learning-based skin lesion classification for cancer detection," Dec. 2024, doi: 10.21203/rs.3.rs-5675190/v1.
- [27] A. Mahalakshmi, C. Padmavathy, N. Priya, G. Priyanka, L. Babu, and B. Archana, "Skin Cancer Detection Using Deep Learning," Aug. 2024, doi: 10.1109/icees61253.2024.10776866.
- [28] N. L. Devi, D. V. Kumar, N. Silpa, V. V. R. M. Rao, S. M. Padmaja, and S. S. Reddy, "Deep Learning-Based Classification of Skin Lesions for Enhanced Dermatological Diagnosis," Aug. 2024, doi: 10.1109/nmitcon62075.2024.10698908.
- [29] R. Pasumarthy and L. Gondi, "An Extensive Examination of Methods for Detecting and Classifying Malignant and Benign Skin Cancers Using Deep Learning Techniques," Apr. 2024, doi: 10.1109/icdcece60827.2024.10548394.
- [30] V. Rajasekar, N. K., and S. A., "An Intelligent System For Skin Cancer Detection Using Deep Learning Techniques," Apr. 2024, doi: 10.1109/adics58448.2024.10533643.
- [31] S. Afrifa, V. Vijayakumar, P. Appiahene, T. Zhang, D. Gyamfi, and R.-M. O. M. Gyening, "Deep Neural Networks for Skin Cancer Classification: Analysis of Melanoma Cancer Data," *Journal of Advances in Information Technology*, Jan. 2025, doi: 10.12720/jait.16.1.1-11.
- [32] C. Magalhaes, J. Mendes, and R. Vardasca, "Systematic Review of Deep Learning Techniques in Skin Cancer Detection," *BioMedInformatics*, Nov. 2024, doi: 10.3390/biomedinformatics4040121.
- [33] V. Ranjan, K. Chaurasia, and J. Singh, "A Comprehensive Survey of Skin Cancer Identification using Deep Learning," *Recent advances in electrical & electronic engineering*, Jan. 2025, doi: 10.2174/0123520965335638241213141707.